3

Structural studies of phosphoinositide 3-kinase-dependent traffic to multivesicular bodies

David J. Gill*[1], Hsiangling Teo*[1], Ji Sun‡, Olga Perisic*, Dmitry B. Veprintsev†, Yvonne Vallis*, Scott D. Emr‡ and Roger L. Williams*[2]

*MRC Laboratory of Molecular Biology, Medical Research Council Centre, Cambridge, CB2 2QH, U.K., †Centre for Protein Engineering, Medical Research Council Centre, Cambridge, CB2 2QH, U.K., and ‡Department of Cellular and Molecular Medicine, The Howard Hughes Medical Institute, University of California, San Diego, School of Medicine, La Jolla, CA 92093-0668, U.S.A.

Abstract

Three large protein complexes known as ESCRT I, ESCRT II and ESCRT III drive the progression of ubiquitinated membrane cargo from early endosomes to lysosomes. Several steps in this process critically depend on PtdIns3P, the product of the class III phosphoinositide 3-kinase. Our work has provided insights into the architecture, membrane recruitment and functional interactions of the ESCRT machinery. The fan-shaped ESCRT I core and the trilobal ESCRT II core are essential to forming stable, rigid scaffolds that support additional, flexibly-linked domains which serve as gripping tools for recognizing elements of the MVB (multivesicular body) pathway: cargo protein, membranes and other MVB proteins. With these additional (non-core) domains, ESCRT I grasps monoubiquitinated membrane proteins and the Vps36 subunit of the downstream ESCRT II complex. The GLUE domain extending beyond the core of the ESCRT II complex recognizes PtdIns3P-containing membranes, monoubiquitinated cargo and ESCRT I. The structure of this GLUE domain demonstrates that it has a split PH (pleckstrin homology) domain fold, with a non-typical phosphoinositide-binding pocket. Mutations in the lipid-binding pocket of the ESCRT II GLUE domain cause a strong defect in vacuolar protein sorting in yeast.

[1]These authors contributed equally to the work. [2]To whom correspondence should be addressed (emial rlw@mrc-lmb.cam.ac.uk).

Introduction

Several pathways of transport to lysosomes have been characterized: AP-3 dependent traffic from the TGN, autophagy, CVT (cytosol-to-vacuole) transport and transport via MVBs (multivesicular bodies). Our structural studies have focused on the molecular mechanisms of traffic to lysosomes via MVBs. This pathway enables transport of monoubiquitinated membrane proteins destined for degradation or action in lysosomes. The MVB pathway can be dissected into several distinct steps: sorting cargo for inclusion into the internalized vesicles, invagination of the endosomal membrane to form internal vesicles, fission of the vesicles from the endosomal membrane, maturation of the MVB through remodelling of the protein and lipid content of the limiting membrane, fusion of the MVB with the lysosome and finally degradation of the lysosomal contents. Some of these steps are dependent on PI3K (phosphoinositide 3-kinase) products, particularly PtdIns3P and PtdIns(3,5)P_2. In yeast, these steps are also dependent on the 18 class E Vps proteins [1]. In mammalian cells, a more complex picture is emerging which suggests that the formation of internal vesicles does not require all of the class E homologues [2,3]. PtdIns3P is abundant on endosomal membranes and the internal vesicles of MVBs [4] and its formation is necessary for the generation of MVB internal vesicles. The enzyme involved in production of 3-phosphoinositides are PI3Ks, which phosphorylate 3-OH group of inositol lipids. Yeast has a single PI3K, Vps34, which is essential for protein sorting and formation of MVBs [5]. However, in mammalian cells, the PI3Ks can be divided into three classes based on the sequences of their catalytic subunits and their associated adaptor subunits. Through microinjection of inhibitory anti-PI3K antibodies, it has been possible to identify the PI3Ks that affect MVB formation and sorting [6–8]. These studies suggest that p110β has a role in early endosomal stages, and that Vps34 is important in later endosomes. Inhibition of hVps34 either by antibodies or by gene silencing precludes the formation of internal vesicles within endosomes but does not prevent fusion with lysosomes [7,9]. Knockdown of hVps34 reduces PtdIns3P associated with late endosomes, yet PtdIns3P-dependent localization is still observed for early endosomes, suggesting that other PI3Ks, possibly in conjunction with polyphosphoinositide phosphatases may be able to compensate for the loss of hVps34 in early endosomes [8,9]. One of the roles of PtdIns3P in endosomal traffic is binding to specific recognition modules and recruitment of endosomal machinery. These recognition modules include FYVE domains and PX (Phox homology) domains. We have recently shown that a type of PH (pleckstrin homology) domain known as a GLUE domain is another PtdIns3P recognition module that is important for endosomal traffic in yeast [10].

Ten of the yeast class E Vps proteins organize into the ESCRT complexes, ESCRT I, ESCRT II and ESCRT III (reviewed by Hurley and Emr [11]). Formation of MVBs in yeast requires Vps27, a protein that has recognition elements for PtdIns3P (a FYVE domain), ubiquitin (a UIM domain), clathrin (a di-leucine clathrin box) and ESCRT I [a P(S/T)XP motif in the C-terminus of Vps27]. The Vps27/ESCRT I interaction in yeast is necessary to recruit ESCRT I to endosomes [12,13]. The assumption of sequential cargo transport

from Vps27 to ESCRT I and ESCRT II in yeast is supported by the observation that overexpression of ESCRT II can partially compensate for sorting defects produced by deletion of ESCRT I subunits [14]. However, this simple picture has been called into question in mammalian cells by the observation that siRNA (small interfering RNA) silencing of ESCRT II subunits had no impact on EGFR (epidermal growth factor receptor) sorting to lysosomes [15]. These results suggest that the role of ESCRT II may be cargo or pathway specific in mammalian cells. Recent structural studies have begun to help decipher the molecular mechanisms of ESCRT complex functions. The primary purpose of this report is to summarize recent structural results concerning the ESCRT I and II complexes and the role of PtdIns3P in ESCRT function.

ESCRT I interacts with monoubiquitinated cargo

Yeast ESCRT I consists of Vps23, Vps28 and Vps37 subunits [16,17]. The human homologues of these proteins are Tsg101, hVps28 and one of Vps37A, Vps37B, Vps37C or Vps37D [18–21]. The Vps23/Tsg101 component of ESCRT I can recognize both ubiquitinated proteins and Vps27/Hrs through its N-terminal UEV domain, and these interactions are crucial to the role of ESCRT-I in cargo sorting. Structural studies of Vps23 [22] and Tsg101 [23] UEV domains bound to ubiquitin have shown that the UEV interacts with a surface centred on Ile[44] of ubiquitin (Figure 1). This partially overlaps with the region of ubiquitin interacting with the UIMs of Vps27 and Hrs [24–26], eliminating the possibility of simultaneous interaction with the same monoubiquitinated cargo.

The role of ESCRT I does not appear to be strictly limited to sorting cargo into internal vesicles. Silencing Tsg101 expression with siRNA results in abnormal endosomes either tubular or with abundant cisternae but with an almost complete lack of internal vesicles [27,28]. The abnormal endosomes are depleted of clathrin, despite the presence of Hrs, leading to speculation that binding Tsg101 may expose the clathrin-interacting region in the C-terminus of Hrs.

The ESCRT I core is built of three helical hairpins splayed as a fan

Using limited proteolysis and sequence analysis we defined and structurally characterized the *Saccharomyces cerevisiae* ESCRT I core. The heterotrimeric complex consists of a single copy each of the C-terminal regions of Vps23 (residues 305–385) and Vps37 (residues 130–213), and the N-terminal region of Vps28 (residues 1–147). The structure of the ESCRT I core was determined independently by James Hurley and his colleagues and by us [10,29].

Each of the subunits in the core contains a helical hairpin of about 60 residues, which tightly pack against each other to generate a rigid, fan-like arrangement. Vps23 is the middle rib of the fan making direct interactions with the Vps28 subunit on one side and the Vps37 subunit on the other (Figure 1). There are no direct interactions between Vps28 and Vps37. The loops of the three hairpins
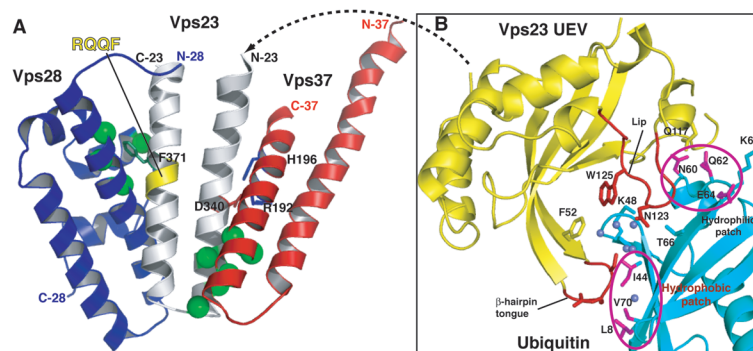
Figure 1 The structure of the ESCRT I.
(A) The rigid ESCRT I core consisting of Vps23 (residues 305–385), Vps28 (residues 1–147) and Vps37 (residues 130–213) serves as a scaffold for additional flexibly linked domains that carry out various functions. The ESCRT I core is largely held together by hydrophobic interactions (green spheres). Two key interacting regions are highlighted: the conserved $R^{368}QQF^{371}$ motif of Vps23 central to the Vps23/Vps28 interface and the conserved salt link at the Vps23/Vps37 interface. **(B)** A detailed view of the interactions of the Vps23 UEV domain with ubiquitin. The ubiquitin is grasped between two loops, the β-hairpin tongue and the lip (red). The interactions on the ubiquitin face can be divided into two regions, a predominantly hydrophobic region that also interacts with the Vps27 UIM domains and a hydrophilic region that is unique to the UEV/ubiquitin interaction.

form the pivot of the fan, while the N- and C-termini of the hairpins radiate from the outer rim. The C-terminus of Vps28 has three additional small helices that fold back and pack against its own hairpin.

Most of the intersubunit interactions are hydrophobic, with only a few notable salt links, one at the centre of the Vps23/Vps28 interface and one central to the Vps23/Vps37 interface (Figure 1). A $R^{368}QQF^{371}$ motif from Vps23 is part of a ball-and-socket type of interaction formed by the side chain of Phe^{371,Vps23} fitting into a hydrophobic pocket on Vps28 lined with side chains of Ile^{37}, Leu^{40}, Tyr^{44}, and Tyr^{104}. Mutation of the tetrapeptide analogous to the $R^{368}QQF^{371}$ motif in human Tsg101 ($R^{368}KQF^{371}$) abrogates the Tsg101/hVps28 interaction and the role of ESCRT-I in viral budding [30]. The Vps23/Vps37 interface is anchored by hydrophobic interactions at the stem of the fan, and further reinforced by salt links of invariant Asp^{340,Vps23} with conserved Arg^{192,Vps37} and His^{196,Vps37}. These basic residues are part of the most conserved sequence motif in Vps37, R^{192}/KXXXHXRR^{199} (where X is any amino acid). Mutations of key ESCRT I interface residues cause strong sorting defects *in vivo* [29].

When Tsg101 is knocked down with siRNA, there is a concomitant decrease in the levels of Vps28, suggesting that the subunits form a constitutive, stable complex in cells [27]. A region at the C-terminus of Tsg101 that was named the 'steadiness box', residues 346–390, was shown previously to be critical for the stability of ESCRT I. This region maps to the Vps23 hairpin central to the packing of ESCRT-I core. The 1:1:1 stoichiometry of the ESCRT I core led us

to re-examine the composition of the full-length complex, which behaves as a 350 kDa complex when isolated from yeast [16,17]. Analytical equilibrium ultracentrifugation of the ESCRT I complex expressed in *Escherichia coli* shows an average apparent molecular mass of approx. 105 kDa, close to the expected size for a 1:1:1 complex (94.7 kDa). The presence of a minor heavier species could represent a small fraction of dimeric ESCRT I. The 350 kDa estimate based on gel filtration could be the consequence of either the non-globular shape of the complex or regulated oligomerization in yeast.

The ESCRT II core forms a trilobal heterotetramer

The structure of the ESCRT II core shows that the complex contains two copies of Vps25 and one copy each of Vps22 and Vps36 [31,32]. The complex has a trilobal shape, with two lobes corresponding to two molecules of Vps25 and one lobe representing the tightly-packed Vps22 and Vps36 subunits (Figure 2). In the crystal structure, the N-terminal 395 residues for Vps36 and residues 1–21 of Vps22 are not visible. Each subunit in the complex has two repeats of a structural module known as a WH (winged-helix) domain, arranged head-to-tail, giving each subunit an oblong shape. Although the three ESCRT II subunits have no recognizable sequence similarity, all eight WH domains in the ESCRT II complex superimpose on each other with an root mean square deviation less than 2 Å (1 Å=0.1 nm). The two Vps25 subunits make no direct contacts with each other. Instead, one Vps25 subunit contacts Vps22, and the other Vps25 contacts Vps36. The structure of the isolated Vps25 subunit shows a conformation essentially identical with the conformation of this subunit in the ESCRT II complex [33].

The N terminus of Vps25 includes two conserved PPXY motifs, P5PVY8 and P11PLY14. PPXY motifs in other proteins are often ligands for WW domains, and the Rsp5/Nedd4 ubiquitin ligase can be recruited by PPXY motifs [34–36]. However, in ESCRT II, these motifs are involved in intermolecular contacts within the complex. Both PPXY motifs from one Vps25 make hydrophobic interactions with Vps22, and very similar interactions are made between the second copy of Vps25 and Vps36 (Figure 2). These two PPXY motifs flank the strictly conserved Phe10,Vps25, which fits as a hydrophobic ball into a hydrophobic socket on the surface of Vps22 or Vps36 and is central to the intersubunit interfaces [31,32]. The Vps22 and Vps36 subunits pair side by side, and form extensive contacts with each other. The mutational analysis of key interactions between the ESCRT II subunits carried out by Emr's and Hurley's groups shows that their disruption leads to cargo mis sorting and class E phenotype in yeast [31].

The helix at the N terminus of Vps22 that extends away from the body of the complex forms part of the N terminal five helix domain of Vps22 (residues 22–90). This N terminal extension of Vps22 has a conserved patch on its surface (Figure 2) that cries out for a binding partner but, so far none has been identified.
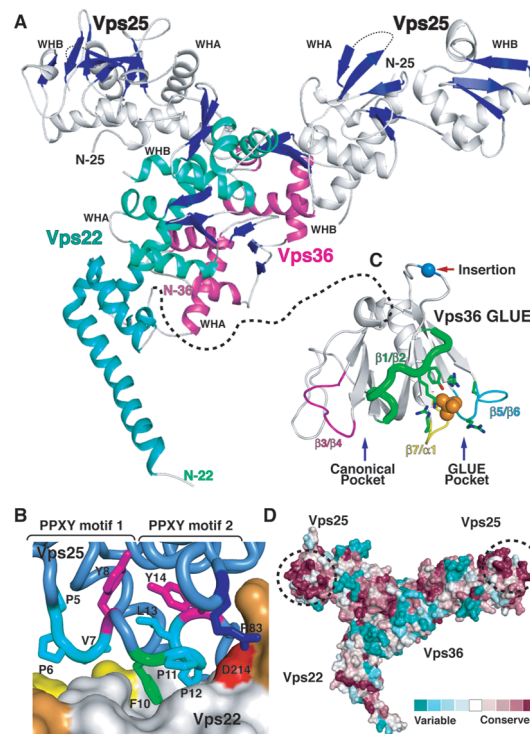
Figure 2 The ESCRT II core forms a trilobal heterotetramer.
(A) ESCRT II core contains two copies of Vps25 and one copy each of Vps22 and Vps36. Each subunit has two tandem repeats of the same building block, a winged helix domain (WHA and WHB). **(B)** The two tandem PPXY motifs near the N-terminus of Vps25 are buried and form very similar interactions with the Vps22 (shown in this Figure) and Vps36. Therefore these motifs cannot interact with molecules outside the ESCRT II complex. **(C)** The Vps36 GLUE domain has a PH domain fold. The sulfate ion (orange spheres) occupies a phosphoinositide binding pocket that is on a different side of the β1/β2 loop (thick green tube), opposite of the canonical pocket commonly found in PH domains. **(D)** Surface mapping of conserved residues in ESCRT II using Consurf [53] reveals a conserved patch in Vps25 which might interact with Vps20 (ESCRT III).

ESCRT II (Vps25 subunit) interacts directly with Vps20 subunit of ESCRT III

A variety of interactions among ESCRT complexes have been demonstrated in vivo, and these interactions are important for the sequential process of cargo sorting [14,37–39]. Using purified proteins, a direct, specific interaction between Vps25 (ESCRT II) and Vps20 (ESCRT III) has been demonstrated [32,40].

The structure of the ESCRT II complex shows that much of the Vps25 surface is accessible for interactions, with exposed, conserved patches that might bind other proteins such as Vps20 (Figure 2). It has been noted that the WHB

domains of the Vps25 subunits, which protrude away from the core of the ESCRT II complex, have a prominent negatively charged face that also could form part of the interaction with Vps20 [33].

The ESCRT II GLUE domain is a hub of binding activity

The N-terminal region of Vps36 subunit, which was not ordered in the crystal structure of the full length ESCRT II, was predicted to contain a PH domain interrupted by a large, 150-residue NZF-containing insertion [10,41]. Such domain-within-domain insertions are observed in approx. 10% of proteins whose structures have been determined [42], and this may be a relatively common occurrence for PH domains as compared with other domains. The GLUE domain from both human [41] and yeast [10] Vps36 bind 3-phosphoinositides *in vitro*. For the yeast GLUE domain, the PtdIns3*P* binding affinity is approx. 100 nM [10].

The crystal structure of the yeast Vps36 GLUE domain from which the 150 residue insertion was removed reveals a typical PH domain architecture with two curved β-sheets and one long α-helix that covers a hydrophobic core between the β-sheets (Figure 2). Although split PH domains have been proposed previously [43], it is only recently that these modules have been structurally characterized [10,44,45]. These structures suggest that the inserted domains do not perturb the canonical PH domain fold. They also show that the inserted domains can be accommodated in more than one of the loops of the domain. Whereas the split PH domains of α-syntrophin and phospholipase C-γ1 have a domain inserted in the region between strands β3 and β4, the Vps36 GLUE domain has the zinc fingers inserted between strands β6 and β7. The insertion of the PDZ domain in the α-syntrophin PH domain increase the avidity for phosphoinositide-containing membranes. In contrast, the insertion of the NZF domains in the GLUE domain has little effect on lipid binding.

The yeast GLUE domain has a positively charged pocket which is occupied by a single sulfate anion in the crystal structure. The walls of the pocket are built by three loops, β1/β2, β5/β6 and β7/α1. Mutagenesis of the residues interacting with the sulphate ion eliminates lipid binding, suggesting that the sulphate may mimic the position of the 3-phosphate of PtdIns3*P* when bound to the domain. Modelling of PtdIns3*P* into this pocket suggests that Arg[89] and Arg[261] are putative ligands of the 3-phosphate and that Lys[38] and Arg[86] also form a part of this pocket (Figures 2 and 3). This Vps36 GLUE phosphoinositide pocket is distinct from the pocket between the β1/β2, β3/β4 and β6/β7 loops used by the vast majority of characterized PH domains (Figure 2) [46,47]. However, the PH domains of β-spectrin [48] and the Tfb1/p62 subunit of TFIIH [49], also bind phosphoinositides in a pocket involving loops β5/β6 and β7/α1, on the opposite side of the β1/β2 'fence'.

ESCRT I interacts directly with ESCRT II

Yeast two-hybrid studies have identified interactions between ESCRT I and ESCRT II [37,39]. We have examined ESCRT I–ESCRT II interactions using recombinant complexes *in vitro* to determine whether these interactions are direct. Analytical gel filtration for yeast ESCRT I and ESCRT II shows that the complexes form a direct, stable 'super-complex' *in vitro* [10]. We have mapped the interacting regions to the C-terminus of Vps28 (ESCRT I subunit, residues 148–242) and the N-terminus of Vps36 (ESCRT II subunit, residues 1–289). A deletion variant of the Vps36 GLUE domain lacking a yeast-specific insertion from 100–251 was not able to form a complex with ESCRT I, but this insertion alone is sufficient for the interaction. This yeast-specific insertion in the Vps36 GLUE domain contains two zinc fingers (NZF-N and NZF-C). Only the
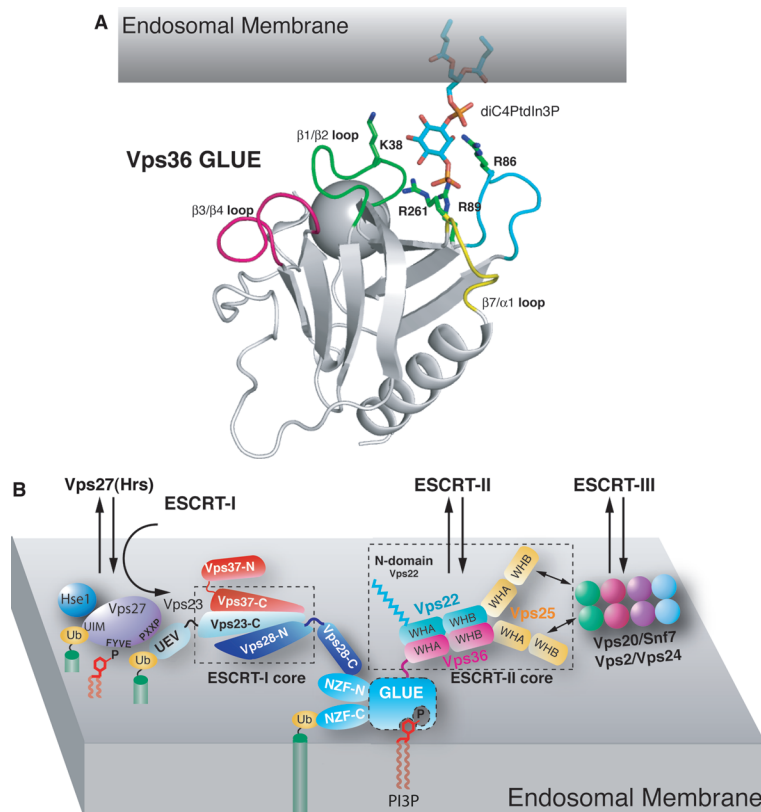

Figure 3 A model of ESCRT I–ESCRT II complex on a membrane.
(A) A model of the PtdIns3*P* bound to the Vps36 GLUE domain based on the sulfate in the crystal structure and mutagenesis. The double zinc-finger region (represented as a large grey sphere) is a yeast-specific insertion between strands β6 and β7. **(B)** A schematic of the assembly of ESCRT complexes on endosomal membranes. An ESCRT I–ESCRT II super-complex on membranes acts to effectively couple interactions with cargo, lipids and sorting machinery.

isolated GST-NZF-N binds to the Vps28 C-terminus. Therefore the two NZF fingers from Vps36 have different functions: NZF-N binds to ESCRT I [10] and NZF-C binds to ubiquitin [50]. The GLUE domain of yeast Vps36 therefore appears to support a remarkable range of functions: binding of ubiquitin to facilitate sorting of monoubiquitinated cargo proteins, interaction with Vps28 of ESCRT I, and binding to 3-phosphoinositide-containing membranes. All of these interactions can function simultaneously [10]. The mammalian Vps36 was also shown to bind ubiquitin [41].

The strong ESCRT I–ESCRT II interaction seen for the recombinant yeast complexes *in vitro* is not apparent in complexes isolated from yeast, suggesting that formation of this super-complex may be regulated in yeast.

Conclusions

Although great progress has been made in understanding the yeast ESCRT I and II complexes in structural terms, there is much that remains unknown. Is the ESCRT I/ESCRT II interaction regulated *in vivo*, and how? What is the link between metazoan ESCRT I/ESCRT II? The metazoan Vps36 GLUE domain has no zinc-finger insertion, nevertheless, it is capable of interacting with both 3-phosphoinositides and ubiquitin [41]. The lack of structural information about any of the ESCRT III subunits impedes understanding of the final stages of MVB formation and Vps4-dependent disassembly of MVB machinery. How do various ESCRT components link to other processes such as pH regulation of gene expression [51] or retrovirus budding [52]?

There is a growing appreciation for the differences between the yeast and the mammalian ESCRT pathways. The disparities are especially acute for the ESCRT III subunits. Although there are six yeast ESCRT III-related subunits in yeast (four of which have been referred to as the core subunits, Vps2, Vps20, Vps24 and Snf7), humans have ten subunits. In yeast, formation of internal vesicles requires ESCRT III subunits, whereas studies in mammalian cells suggest that ESCRT III subunits are important for the fusion of the MVBs with lysosomes and receptor degradation, but that internal vesicles can be formed in the absence of at least some ESCRT III components [2,3].

References

1.   Babst, M. (2005) Traffic **6**, 2–9
2.   Shim, J.H., Xiao, C., Hayden, M.S., Lee, K.Y., Trombetta, E.S., Pypaert, M., Nara, A., Yoshimori, T., Wilm, B., Erdjument-Bromage, H. et al. (2006) J. Cell. Biol. **172**, 1045–1056
3.   Bache, K.G., Stuffers, S., Malerod, L., Slagsvold, T., Raiborg, C., Lechardeur, D., Walchli, S., Lukacs, G.L., Brech, A. and Stenmark, H. (2006) Mol. Biol. Cell **17**, 2513–2523
4.   Gillooly, D.J., Morrow, I.C., Lindsay, M., Gould, R., Bryant, N.J., Gaullier, J.M., Parton, R.G. and Stenmark, H. (2000) EMBO J. **19**, 4577–4588
5.   Schu, P.V., Takegawa, K., Fry, M.J., Stack, J.H., Waterfield, M.D. and Emr, S.D. (1993) Science **260**, 88–91
6.   Siddhanta, U., McIlroy, J., Shah, A., Zhang, Y. and Backer, J.M. (1998) J. Cell Biol. **143**, 1647–1659
7.   Futter, C.E., Collinson, L.M., Backer, J.M. and Hopkins, C.R. (2001) J. Cell Biol. **155**, 1251–1264

8. Shin, H.W., Hayashi, M., Christoforidis, S., Lacas-Gervais, S., Hoepfner, S., Wenk, M.R., Modregger, J., Uttenweiler-Joseph, S., Wilm, M., Nystuen, A. et al. (2005) J. Cell Biol. **170**, 607–618
9. Johnson, E.E., Overmeyer, J.H., Gunning, W.T. and Maltese, W.A. (2006) J. Cell Sci. **119**, 1219–1232
10. Teo, H., Gill, D.J., Sun, J., Perisic, O., Veprintsev, D.B., Vallis, Y., Emr, S.D. and Williams, R.L. (2006) Cell **125**, 99–111
11. Hurley, J.H. and Emr, S.D. (2006) Annu. Rev. Biophys. Biomol. Struct. **35**, 277–298
12. Katzmann, D.J., Stefan, C.J., Babst, M. and Emr, S.D. (2003) J. Cell Biol. **162**, 413–423
13. Bilodeau, P.S., Winistorfer, S.C., Kearney, W.R., Robertson, A.D. and Piper, R.C. (2003) J. Cell Biol. **163**, 237–243
14. Babst, M., Katzmann, D.J., Snyder, W.B., Wendland, B. and Emr, S.D. (2002) Dev. Cell **3**, 283–289
15. Bowers, K., Piper, S.C., Edeling, M.A., Gray, S.R., Owen, D.J., Lehner, P.J. and Luzio, J.P. (2006) J. Biol. Chem. **281**, 5094–5105
16. Babst, M., Odorizzi, G., Estepa, E.J. and Emr, S.D. (2000) Traffic **1**, 248–258
17. Katzmann, D.J., Babst, M. and Emr, S.D. (2001) Cell **106**, 145–155
18. Bishop, N. and Woodman, P. (2001) J. Biol. Chem. **276**, 11735–11742
19. Stuchell, M.D., Garrus, J.E., Muller, B., Stray, K.M., Ghaffarian, S., McKinnon, R., Krausslich, H.G., Morham, S.G. and Sundquist, W.I. (2004) J. Biol. Chem. **279**, 36059–36071
20. Bache, K.G., Slagsvold, T., Cabezas, A., Rosendal, K.R., Raiborg, C. and Stenmark, H. (2004) Mol. Biol. Cell **15**, 4337–4346
21. Eastman, S.W., Martin-Serrano, J., Chung, W., Zang, T. and Bieniasz, P.D. (2005) J. Biol. Chem. **280**, 628–636
22. Teo, H., Veprintsev, D.B. and Williams, R.L. (2004) J. Biol. Chem. **279**, 28689–28696
23. Sundquist, W.I., Schubert, H.L., Kelly, B.N., Hill, G.C., Holton, J.M. and Hill, C.P. (2004) Mol. Cell **13**, 783–789
24. Bilodeau, P.S., Urbanowski, J.L., Winistorfer, S.C. and Piper, R.C. (2002) Nat. Cell Biol. **4**, 534–539
25. Fisher, R.D., Wang, B., Alam, S.L., Higginson, D.S., Robinson, H., Sundquist, W.I. and Hill, C.P. (2003) J. Biol. Chem. **278**, 28976–28984
26. Hirano, S., Kawasaki, M., Ura, H., Kato, R., Raiborg, C., Stenmark, H. and Wakatsuki, S. (2006) Nat. Struct. Mol. Biol. **13**, 272–277
27. Doyotte, A., Russell, M.R., Hopkins, C.R. and Woodman, P.G. (2005) J. Cell Sci. **118**, 3003–3017
28. Razi, M. and Futter, C.E. (2006) Mol. Biol. Cell **17**, 3469–3483
29. Kostelansky, M.S., Sun, J., Lee, S., Kim, J., Ghirlando, R., Hierro, A., Emr, S.D. and Hurley, J.H. (2006) Cell **125**, 113–126
30. Martin-Serrano, J., Zang, T. and Bieniasz, P.D. (2003) J. Virol. **77**, 4794–4804
31. Hierro, A., Sun, J., Rusnak, A.S., Kim, J., Prag, G., Emr, S.D. and Hurley, J.H. (2004) Nature **431**, 221–225
32. Teo, H., Perisic, O., Gonzalez, B. and Williams, R.L. (2004) Dev. Cell **7**, 559–569
33. Wernimont, A.K. and Weissenhorn, W. (2004) BMC Struct. Biol. **4**, 10
34. Dunn, R. and Hicke, L. (2001) Mol. Biol. Cell **12**, 421–435
35. Katzmann, D.J., Sarkar, S., Chu, T., Audhya, A. and Emr, S.D. (2004) Mol. Biol. Cell **15**, 468–480
36. Stimpson, H.E., Lewis, M.J. and Pelham, H.R. (2006) EMBO J. **25**, 662–672
37. Bowers, K., Lottridge, J., Helliwell, S.B., Goldthwaite, L.M., Luzio, J.P. and Stevens, T.H. (2004) Traffic **5**, 194–210
38. Martin-Serrano, J., Yarovoy, A., Perez-Caballero, D. and Bieniasz, P.D. (2003) Proc. Natl. Acad. Sci. U.S.A. **100**, 12414–12419
39. von Schwedler, U.K., Stuchell, M., Muller, B., Ward, D.M., Chung, H.Y., Morita, E., Wang, H.E., Davis, T., He, G.P., Cimbora, D.M. et al. (2003) Cell **114**, 701–713
40. Yorikawa, C., Shibata, H., Waguri, S., Hatta, K., Horii, M., Katoh, K., Kobayashi, T., Uchiyama, Y. and Maki, M. (2005) Biochem. J. **387**, 17–26
41. Slagsvold, T., Aasland, R., Hirano, S., Bache, K.G., Raiborg, C., Trambaiolo, D., Wakatsuki, S. and Stenmark, H. (2005) J. Biol. Chem. **280**, 19600–19606
42. Aroul-Selvam, R., Hubbard, T. and Sasidharan, R. (2004) J. Mol. Biol. **338**, 633–641

43. Lemmon, M.A. (2005) Cell **120**, 574–576
44. Wen, W., Yan, J. and Zhang, M. (2006) J. Biol. Chem. **281**, 12060–12068
45. Yan, J., Wen, W., Xu, W., Long, J.F., Adams, M.E., Froehner, S.C. and Zhang, M. (2005) EMBO J. **24**, 3985–3995
46. Ferguson, K.M., Kavran, J.M., Sankaran, V.G., Fournier, E., Isakoff, S.J., Skolnik, E.Y. and Lemmon, M.A. (2000) Mol. Cell **6**, 373–384
47. Lietzke, S.E., Bose, S., Cronin, T., Klarlund, J., Chawla, A., Czech, M.P. and Lambright, D.G. (2000) Mol. Cell **6**, 385–394
48. Hyvönen, M., Macias, M.J., Nilges, M., Oschkinat, H., Saraste, M. and Wilmanns, M. (1995) EMBO J. **14**, 4676–4685
49. Di Lello, P., Nguyen, B.D., Jones, T.N., Potempa, K., Kobor, M.S., Legault, P. and Omichinski, J.G. (2005) Biochemistry **44**, 7678–7686
50. Alam, S.L., Sun, J., Payne, M., Welch, B.D., Blake, B.K., Davis, D.R., Meyer, H.H., Emr, S.D. and Sundquist, W.I. (2004) EMBO J. **23**, 1411–1421
51. Penalva, M.A. and Arst, Jr, H.N. (2004) Annu. Rev. Microbiol. **58**, 425–451
52. Morita, E. and Sundquist, W.I. (2004) Annu. Rev. Cell Dev. Biol. **20**, 395–425
53. Glaser, F., Pupko, T., Paz, I., Bell, R.E., Bechor-Shental, D., Martz, E. and Ben-Tal, N. (2003) Bioinformatics **19**, 163–164